# Impact of Brillouin amplification on the spatial resolution of noise-correlated Brillouin optical reflectometry

**Mingjiang Zhang (张明江)[1,2,3,*], Xiaoyi Bao (鲍晓毅)[3], Jing Chai (柴 晶)[1,2], Yongning Zhang (张永宁)[1,2], Ruixia Liu (刘瑞霞)[1,2], Hui Liu (刘 慧)[1,2], Yi Liu (刘 毅)[1,2], and Jianzhong Zhang (张建忠)[1,2]**

[1]*Key Lab of Advanced Transducers and Intelligent Control Systems, Ministry of Education and Shanxi Province, Taiyuan 030024, China*

[2]*Institute of Optoelectronic Engineering, College of Physics & Optoelectronics, Taiyuan University of Technology, Taiyuan 030024, China*

[3]*Fiber Optics Group, Department of Physics, University of Ottawa, Ottawa K1N 6N5, Canada*

**Corresponding author: zhangmingjiang@tyut.edu.com*

Received January 24, 2017; accepted April 21, 2017; posted online May 12, 2017

To obtain high spatial resolution over a long sensing distance in Brillouin optical correlation domain reflectometry (BOCDR), a broad laser spectrum and high pump power are used to improve the signal-to-noise ratio (SNR). In this Letter, we use a noise-modulated laser to study the variation of the Brillouin spectrum bandwidth and its impact on the coherent length of BOCDR quantitatively. The result shows that the best spatial resolution (lowest coherent length) is achieved by the lowest pump power with the highest noise-modulation spectrum. Temperature-induced changes in the Brillouin frequency shift along a 253.1 m fiber are demonstrated with a 19 cm spatial resolution.

*OCIS codes: 060.2370, 060.4080, 120.5820, 290.5830.*
*doi: 10.3788/COL201715.080603.*

Distributed optical fiber sensors have been widely used to monitor temperature[1,2], strain[3], vibration[4], and so on. Specifically, the sensors based on Brillouin scattering have been studied extensively to measure the strain or temperature along an optical fiber[5–7]. Brillouin optical time-domain reflectometry (BOTDR) based on spontaneous Brillouin scattering[8–10] and Brillouin optical time-domain analysis (BOTDA) based on stimulated Brillouin scattering[11–14] both require optical pulses to realize the distributed measurement. Based on a continuous wave (CW) in reflection mode, Brillouin optical correlation domain reflectometry (BOCDR)[15–18] and, in counterpropagating mode, Brillouin optical correlation domain analysis (BOCDA)[19] are proposed in which spatial information is obtained by changing the modulation frequency via Fourier analysis, and a Brillouin frequency shift (BFS) is achieved by sweeping a Brillouin spectrum. A BOCDR or BOCDA system is based on the sine wave modulating the pump light, probe light, or reference light, and the limited frequency range over a finite time limits the sensing length and spatial resolution[15,19]. Recently, in order to circumvent the limitation in the BOCDA[20–22], the probe light and reference light were phase modulated by a common binary pseudo-random bit sequence (PRBS) and a distance of 200 m was measured with a 1 cm resolution[20]. Moreover, a broadband laser source based on the amplified spontaneous emission (ASE) of an erbium-doped optical fiber amplifier (EDFA) was used in the BOCDA system, and a spatial resolution of 4 mm was obtained over a 5 cm optical fiber[21]. Combining temporal gating of the pump with time-domain acquisition in a phase-modulation BOCDA system, a spatial resolution of 8.3 mm was demonstrated over a 17.5 km sensing fiber[22]. Although the BOCDA system can realize a high spatial resolution, the system cannot work completely once the sensing fiber breaks due to two-end access[23]. Thus, the BOCDR with one-end access is more available in some practical applications. In previous work, we used a BOCDR system based on a PRBS-modulated laser source as the probe and reference light to obtain the distribution of temperature along a 250 m optical fiber with a 54 cm spatial resolution[24]. In addition, a slope-assisted BOCDR system was utilized to achieve temperature and strain measurements in the respective 20 cm long section simultaneously, along a length of 5 m[18], and demonstrated that a shift in the power change can still be detected when a strained section is even shorter than the nominal resolution[25]. In addition, by designing the lock-in detection scheme and amplifying a small spontaneous Brillouin signal with a lock-in amplifier in the BOCDR, the signal-to noise ratio (SNR) of the system was enhanced and a 20 cm section with a 7000 strain was clearly measured over a 100 m fiber[26].

In this Letter, we propose and demonstrate a novel partially coherent BOCDR scheme based on a noise-modulated laser diode (LD). The impact of high pump power on the coherence length due to Brillouin amplification is studied quantitatively. Partial coherence is introduced by stimulated Brillouin scattering amplification from high pump power, and such a process leads to lower spatial resolution due to longer coherence length, even though the temperature resolution and sensing length

 

can be increased. The limited measurement range in the BOCDR can be resolved by adjusting the length of the optical delay line. This technique allows fast measurements to be carried out with a single source without frequency locking or a synthesizer. The proposed new scheme is much simpler than conventional BOCDR systems. Because of the low coherent state of a noise-modulated distributed feedback (DFB) LD and the introduction of an optical delay line, the proposed BOCDR system makes a significant improvement in terms of sensing range and spatial resolution compared with previous work[15,24]. In experiments, a spatial resolution of 19 cm is demonstrated along a 253.1 m optical fiber.

Conventional BOCDR systems based on sinusoidal frequency modulation[15] or PRBS phase modulation[20] can produce periodic correlation peaks along the fiber under test (FUT), which limits the sensing length[24,27]. However, due to nonperiodicity of the noise signal, when we use a noise signal to modulate the LD, only one correlation peak is synthesized at one point along the FUT. In principle, the measurement range can be arbitrary as long as the ensemble states are sufficiently large with no repeated states. Figure 1 shows the principle diagram of the correlation process between the Brillouin Stokes light and the reference light. Only the same coherence state between the Brillouin Stokes light and the reference light contributes to generation of the correlation peak, and then a high heterodyne signal output can be obtained. The peak frequency will give the BFS, which is proportional to the change of the temperature or strain in the optical fiber. The single correlation peak between the pump light and reference light can be scanned along the FUT using a variable optical delay line. By measuring the distribution of the BFS along the FUT, the distributed temperature or strain change along the optical fiber can be achieved.

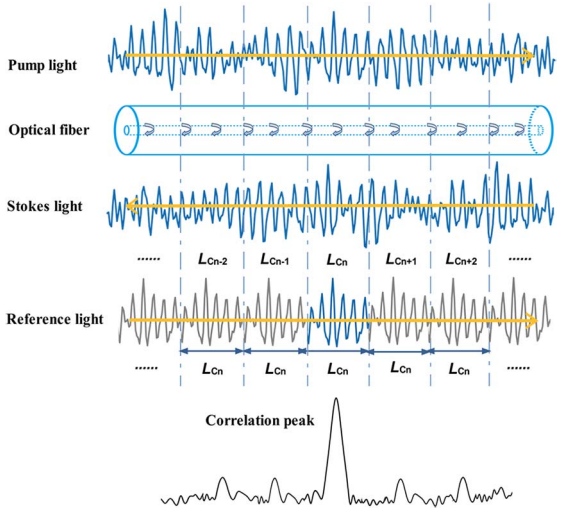


Fig. 1. Principle diagram of the correlation between the Brillouin Stokes light and the reference light.

The spatial resolution of this system is mainly determined by the coherence lengths of Brillouin Stokes light and pump light, which can be very short by controlling the current-modulation parameters of the DFB-LD. As a result, the spatial resolution can be affected by the modulation intensity, namely the power of the noise signal used to modulate the DFB-LD. The spatial resolution of our scheme can be estimated by

$$\Delta z \propto \int_0^T [f_1(t) \cdot f_2(t+\tau)]\mathrm{d}t, \tag{1}$$

where $\Delta z$ is the spatial resolution, $T$ is the lifetime of the acoustical phonon, $f_1$ and $f_2$ are the wave functions of the reference light and Brillouin Stokes light, respectively, and $\tau$ is the delay time between the reference light and Brillouin Stokes light. The changes of the coherence lengths of the reference light and Brillouin Stokes light lead to the variation of the spatial resolution.

The experimental setup of proposed BOCDR based on a noise-modulated laser is depicted in Fig. 2. A DFB-LD with a 1550.28 nm central wavelength was used as the laser source, which was modulated by a noise signal generated by a noise signal generator (NSG). The modulated laser was divided into two branches (pump light and reference light) by a 50∶50 fiber-optic coupler. The pump light was amplified by a high-power erbium-doped fiber amplifier (EDFA1) and later launched into the FUT via an optical circulator (OC). The injection of the pump light beam into the sensing fiber generated the backscattered Brillouin signal (Stokes light) at every point of the FUT.

Then a high-sensitive EDFA3 was used to amplify the Stokes light. To eliminate the noise of ASE, Rayleigh scattering and anti-Stokes light, a narrow bandwidth optical filter was introduced. For another branch, the reference light was transported through a polarization controller (PC) and a programmable optical delay generator (General Photonics, ODG-101), which was used as the variable optical delay line wherein the optical delay range was 20 km, the minimum delay step size was 30 cm, and the delay change speed was 10 ms. Then another EDFA2 was introduced to amplify the reference light in order to enhance the heterodyne beat signal. The variable optical delay line was used to locate the measured position along

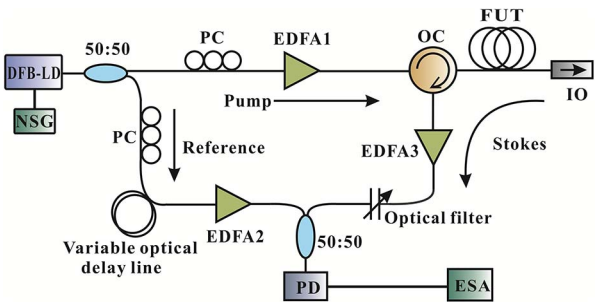


Fig. 2. Experimental setup of the partially coherent BOCDR using a noise-modulated LD.

the 253.1 m FUT, where the temperature was around 23.6°C, and a 9 m section of the sensing fiber was placed in an incubator. The length of the reference light path was adjusted to have the same length as the pump light path so that the backscattered Brillouin Stokes light and the reference light were in the same coherent state when they correlated through a fiber-optic coupler. Thus, we could obtain maximum contrast for the correlation beat signal. The optical beat signal was converted to an electrical signal through a photodiode (PD) and monitored by an electrical spectrum analyzer (ESA). The optical spectra are measured by a high-resolution optical spectrum analyzer with a 0.04 pm resolution. Compared to our previous works[20], a noise-modulated laser source was used as pump light and reference light instead of the PRBS-modulated laser source, which avoids the generation of multiple correlation peaks within the range of FUT.

Figure 3 indicates the characteristics of the noise-modulated DFB-LD. The power and bandwidth of the noise signal have some influences on the linewidth of the DFB-LD. Due to the limitation of the signal generator, we only demonstrate the effect of the power of the noise signal, namely the modulation intensity of the LD. The time sequence of the DFB-LD with the −10 dBm noise modulation power is shown in Fig. 3(a). Figure 3(b) indicates the power spectrum of the DFB-LD with and without noise modulation with the power of −10 dBm. The optical spectra of the DFB-LD under free operation and with different noise modulation powers are shown in Fig. 3(c). Figure 3(d) shows the linewidths and the coherence lengths of the noise-modulated laser with different modulation powers. The linewidth of the noise-modulated DFB-LD impacts the coherence lengths of the pump light and the measurement accuracy of the BFS. With the increase of the modulation intensity of the DFB-LD, the measured Brillouin gain spectrum is broadened and the distortion appears.

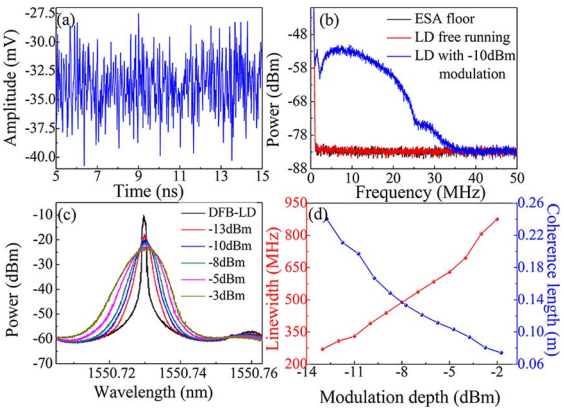


Fig. 3. (Color online) Characteristics of a laser source with the noise-modulation intensity. (a) The time sequence, (b) the power spectra, (c) the optical spectra, and (d) the linewidth and the coherence length versus modulation power.

In the experiment, we first adjusted the optical path of the reference light to make it correlate with the Brillouin Stokes light generated from the heated section in the incubator. By changing the temperature of the incubator, we obtained the BFS versus temperature, and the measured temperature coefficient is 1.05 MHz/°C. Then, keeping the incubator's temperature at 50°C, we adjusted the length of the variable optical delay line to obtain the distribution of the Brillouin spectrum and BFS along the FUT. The distribution of the Brillouin spectrum is illustrated in Fig. 4(a). The Brillouin spectra of the 9 m long heated section are clearly distinguished from other sections of the FUT. Figure 4(b) shows the distribution of the BFS with respect to the fiber length. A frequency shift of about 26 MHz in the BFS is clearly indicated, which agrees well with the applied 26.4°C temperature variation. The accuracy of the measurement at this location is ±1.2 MHz, corresponding to the temperature accuracy of ±1.14°C.

Furthermore, we investigated the spatial resolution of the proposed BOCDR system. The achieved spatial resolution is calculated by averaging the rise and fall time equivalent length in meters for the temperature-changed fiber section[8]. As shown in Fig. 5(a), a spatial resolution of 0.636 m is achieved with a 9 m heated section from 150 to 159 m using noise with an power of −10 dBm to modulate the LD. Figure 5(b) demonstrates that the spatial resolution with −3 dBm noise modulation power can reach 0.19 m along the 253.1 m FUT when a 5 m long section is heated from 189 to 194 m.

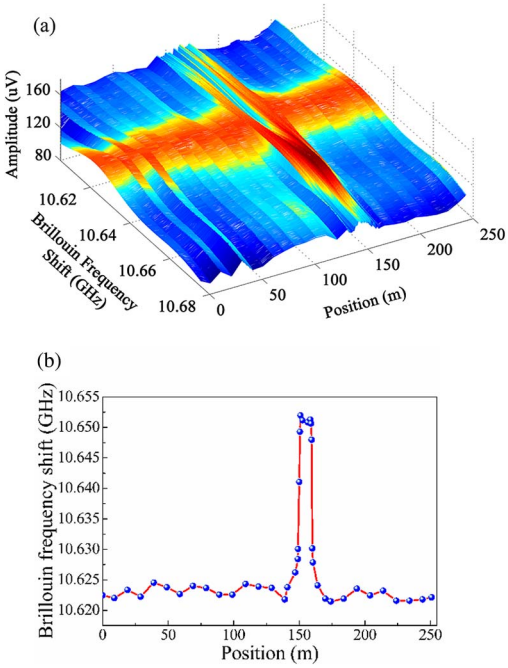


Fig. 4. (Color online) (a) The distribution of the Brillouin spectrum, and (b) the distribution of the BFS along the FUT with a 9 m long heated section.

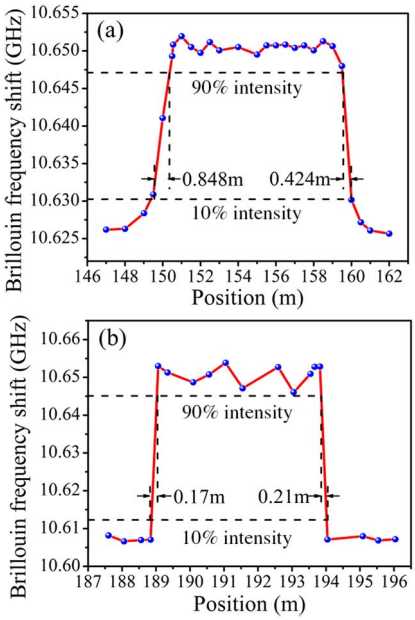


Fig. 5. (Color online) Evaluation of the spatial resolution based on the noise-signal modulation using (rise time + fall time)/2 equivalent length, with (a) a −10 dBm modulation power and (b) a −3 dBm modulation power.

To study the influence of high pump power on the spatial resolution in a BOCDR system, we measured the backscattering light spectra under different pump powers, as shown in Fig. 6, with a −10 dBm noise modulation power for different optical powers from 0.4666 to 1.8870 W. As shown in the illustration of Fig. 6, the −3 dB linewidth of the Brillouin Stokes light decreases from 322.10 to 98.35 MHz when the optical power increases from 0.4666 to 1.8870 W. Even at 466 mW, the Stokes spectrum is narrower than that of the pump light at 389.8 MHz [shown in Fig. 3(d)]. If we look at the intensity of the Stokes light closely, it is much higher than the anti-Stokes peak, which indicates the existence of the Brillouin amplification process. Only under the process of spontaneous Brillouin scattering, i.e., can the intensity of the Stokes and anti-Stokes peaks be equal and the coherence length of the pump light spectrum be equivalent to the spatial resolution.

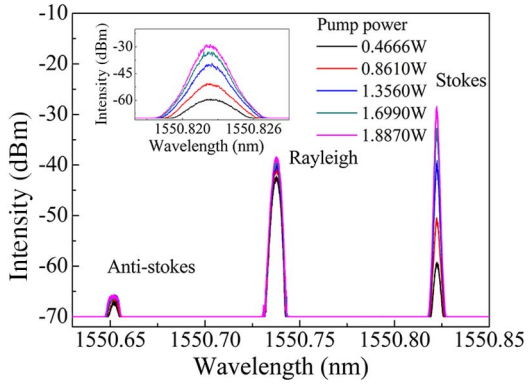


Fig. 6. (Color online) Backscattering light spectra of the pump light with a −10 dBm noise modulation power.

In addition, the coherence lengths of the Brillouin Stokes light with different Brillouin backscattering states also are analyzed and the results are shown in Fig. 7. The coherent length of Brillouin Stokes light is measured when the peak power of Brillouin Stokes light is around −60, −50, −40, −30, and −25 dBm, respectively. The experimental result indicates that, for the same noise modulation power, the coherence length of the Brillouin Stokes light rises slowly with the increase of the peak power of the Brillouin Stokes light. With the increase of the modulation power, the differences of the coherence lengths of the different Brillouin backscattering states becomes smaller. The coherence length of Brillouin Stokes light tends to be close to that of pump light when the modulation power increases.

Finally, we made a comparison between the measured spatial resolution and the calculated coherence lengths of Brillouin Stokes light and pump light with different modulation powers, and obtained the relevant errors by multiple measurements. The results are shown in Fig. 8. The spatial resolution, coherence length of Brillouin Stokes light, and the relevant errors are measured when the peak power of the Brillouin Stokes light is about −50 dBm, which is about 10 dB weaker than that of Rayleigh scattering light. As shown in Fig. 8, for different modulation powers, the measured spatial resolution is always larger than the coherence length of the pump light and the Brillouin Stokes light, which is different with the results in Refs. [11,17].

Figure 8 indicates that the spatial resolution of the partially coherent BOCDR is not equal to the coherence length of the pump light or Brillouin Stokes light. We consider that the spatial resolution of the partially coherent BOCDR scheme is proportional to the convolution between the coherence length of the pump light and that of the Brillouin Stokes light, as given by Eq. (1). Since the coherence length of the Brillouin Stokes light is

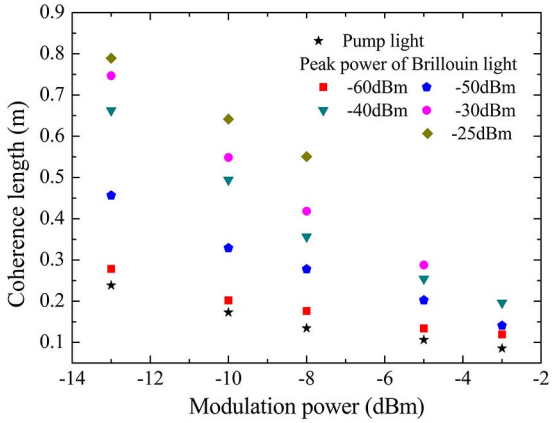


Fig. 7. (Color online) Coherence length of the Brillouin Stokes light as a function of the noise modulation power with different Brillouin backscattering states.

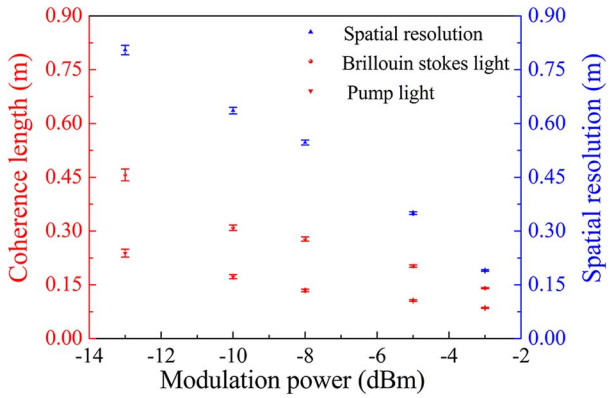


Fig. 8. (Color online) Measured spatial resolution, the coherence lengths of the pump light and Brillouin backscattering Stokes light, and the measured errors under different modulation powers.

dependent on the power and linewidth of the pump light, the spatial resolution will be influenced. As can be seen from Fig. 8, with the increase in the modulation power, the measured spatial resolution and the coherence lengths of the Brillouin Stokes light and the pump light become closer, thus we believe that the spatial resolution and the coherence length of the Brillouin Stokes light will be equal to the coherence length of the pump light if the modulation power is large enough, namely the −3 dB linewidth of pump light is broad enough, which will be the same as the results of Refs. [17,20] in which an incoherent light source is used as the pump light. Furthermore, the spatial resolution of the mm scale will be achieved in the proposed method if a broadband noise signal is adopted to modulate the DFB-LD. However, the mm-scale resolution means that the weak Brillouin scattering signal, hence the low SNR of the system, will limit the sensing range.

In conclusion, a new type of partially coherent BOCDR sensing technique is proposed and demonstrated to study the relationship between the spatial resolution and the coherence lengths of the pump light and the Brillouin Stokes light based on a noise-modulated DFB-LD. The new method ensures a single correlation peak in the entire sensing range due to the nonperiodic states of the reference light and the Brillouin Stokes light, which simultaneously avoids the range limitation of the periodic correlation peaks and maintains the high spatial resolution. A 19 cm spatial resolution and a 253.1 m measurement range are successfully demonstrated. Simpler than conventional Brillouin sensing systems, the proposed scheme makes a cost-effective distributed Brillouin sensing system for a high-accuracy distributed temperature measurement with a high spatial resolution without the need of high speed and a broadband sampling scope for mm or cm spatial resolution.

One of the authors, Mingjiang Zhang, thanks Dr. Liang Zhang and Dr. Dapeng Zhou, University of Ottawa, Canada, and Prof. Yuncai Wang, Taiyuan University of Technology, China, for their helpful discussions and proofreading the manuscript, and also thanks visiting Prof. Huimin Cai, University of Ottawa, Canada, for polishing up the manuscript.

This work was supported by the National Natural Science Foundation of China (Nos. 61377089 and 61527819), the International Science & Technology Cooperation Program of China (No. 2014DFA50870), and the Natural Science Foundation of Shanxi (Nos. 2015011049 and 201601D021069).

## References

1. X. Yan, H. Fu, H. Li, and X. Qiao, Chin. Opt. Lett. **14**, 030603 (2016).
2. Z. Yang, H. Sun, T. Gang, N. Liu, J. Li, F. Meng, X. Qiao, and M. Hu, Chin. Opt. Lett. **14**, 050604 (2016).
3. C. Lin, Y. Wang, Y. Huang, C. Liao, Z. Bai, M. Hou, Z. Li, and Y. Wang, Photon. Res. **5**, 129 (2017).
4. Z. Wang, Z. Pan, Q. Ye, B. Lu, Z. Fang, H. Cai, and R. Qu, Chin. Opt. Lett. **13**, 100603 (2015).
5. X. Bao and L. Chen, Sensors **11**, 4152 (2011).
6. K. Hotate, IEEE Sens. J. **142** (2014).
7. C. K. Y. Leung, K. T. Wan, D. Inaudi, X. Y. Bao, W. Habel, Z. Zhou, J. P. Ou, M. Ghandehari, H. C. Wu, and M. Imai, Mater. Struct. **48**, 871 (2015).
8. D. Garus, E. Geinitz, T. Gogolla, S. Jetschke, K. Krebber, U. Röpke, and S. Unger, in *Optical Fiber Sensors* (1996), Th328.
9. Y. Koyamada, Y. Sakairi, N. Takeuchi, and S. Adachi, IEEE Photon. Technol. Lett. **19**, 1910 (2007).
10. Y. Weng, E. Ip, Z. Pan, and T. Wang, Opt. Express **23**, 9024 (2015).
11. T. Horiguchi and M. Tateda, J. Lightwave Technol. **7**, 1170 (1989).
12. W. Li, X. Bao, Y. Li, and L. Chen, Opt. Express **16**, 21616 (2008).
13. Z. Li and L. Yan, Opt. Express **24**, 4824 (2016).
14. Z. Li, L. Yan, L. Shao, and W. Pan, IEEE Photon. J. **8**, 1 (2016).
15. Y. Mizuno, W. Zou, Z. He, and K. Hotate, Opt. Express **16**, 12148 (2008).
16. N. Hayashi, Y. Mizuno, and K. Nakamura, IEEE Photon. J. **7**, 1 (2015).
17. N. Hayashi, Y. Mizuno, and K. Nakamura, Appl. Phys. Express **7**, 112501 (2014).
18. H. Lee, N. Hayashi, Y. Mizuno, and K. Nakamura, IEEE Photon. J. **8**, 6802807 (2016).
19. K. Y. Song, Z. He, and K. Hotate, Opt. Lett. **31**, 2526 (2006).
20. A. Zadok, Y. Antman, N. Primerov, A. Denisov, J. Sancho, and L. Thevenaz, Laser Photon. Rev. **6**, L1 (2012).
21. R. Cohen, Y. London, Y. Antman, and A. Zadok, Opt. Express **22**, 12070 (2014).
22. A. Denisov, M. A. Soto, and L. Thevenaz, Light Sci. Appl. **5**, e16074 (2016).
23. Y. Mizuno, Z. He, and K. Hotate, Opt. Express **18**, 5926 (2010).
24. J. Chai, M. Zhang, Y. Liu, L. Lan, W. Xu, and Y. Wang, Chin. Opt. Lett. **13**, 080604 (2015).
25. H. Lee, N. Hayashi, Y. Mizuno, and K. Nakamura, Opt. Express **24**, 29191 (2016).
26. Y. G. Yao, M. Kishi, and K. Hotate, Appl. Phys. Express **9**, 072501 (2016).
27. K. Hotate and Z. He, J. Lightwave Technol. **24**, 2541 (2006).